Analytical Methods

Accepted Manuscript

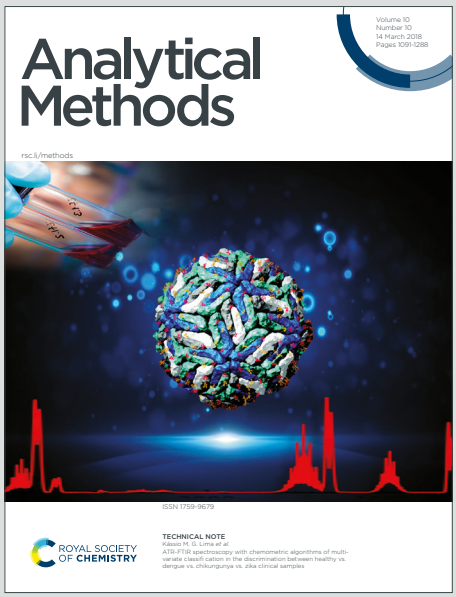

ROYAL SOCIETY OF CHEMISTRY

rsc.li/methods

View Article Online
DOI: 10.1039/D5AY00986C

ARTICLE

Received 00th January 20xx,

Accepted 00th January 20xx

DOI: 10.1039/x0xx00000x

Fluorescence Asymmetry Ratio as an Optical Index of Antioxidant Activity of RP-HPLC Fractions of Fulvic Acids

Anna N. Khreptugova,*[a] Danila M. Gorbunov,[a] Dmitry S. Volkov [a] and Irina V. Perminova [a]

Fulvic acids (FA) have recently gained substantial attention as potential biostimulants within the category of complex carbon-based plant stimulants. However neither preparative technique for isolation of highly active FA components nor quality control demands are formu-lated yet for FA-based biostimulants. The study aims to evaluate antioxidant capacities (AOC) of the FA fractions obtained from the commercial FA material with a use of the preparative RP-HPLC technique and to establish relationships between the AOC values, molecular composi-tion and optical properties in search of the reliable quality control parameters indicating en-hanced AOC values of FA. ABTS assay was used to measure AOC values, high resolution mass spectrometry (HRMS) was applied for molecular composition analysis. More hydrophobic fractions comprised more than 50% of the eluted FA material. They exhibited significantly higher AOC values (0.9-1.4 mmol TE/g) as compared to the more hydrophilic fractions. They were dominated with conjugated tannins – major contributors to the bathochromic shift of the fluorescence spectra. The found close correlation (R^2 = 0.96) between fluorescence asymmetry value (ASM_{350}) and the AOC values highlights the potential of simple one-dimensional fluorescence measurements as a rapid, non-destructive alternative to la-bor-intensive ABTS assays for evaluating antioxidant properties of FA.

1 Introduction

Fulvic acid (FA) is an operationally defined fraction of natural non-living organic matter – humic substances (HS).[1] This fraction remains in the soluble state under acidification below pH 2 of alkaline extract from soil or solid organic rocks (coal, peat, sapropel). The residual portion of HS, which precipitates at pH<2, is called humic acid (HA). By the given definition, FA represents the most oxidized and strongly acidic fraction of HS. It dominates in the composition of natural organic matter (NOM) in the natural aquatic environments comprising up to 90% of the total pool of dissolved organic matter (DOM).[2] It is much less abundant in coal and peat HS: its content varies from 10% (in coal HS) up to 40% (in high moor peat HS), much larger variations are observed in soil HS: from 10-20 in chernozem up to 60-80 in sod podzolic soils. These numbers can be deduced from humification state of these humified substrates measured as a ratio of concentrations of HA to FA in the HS extracts (CHA/CFA).[3–5] Being rich in carboxyl and other oxygen-containing functional groups, FA play important environmental functions. They mediate speciation of metals in aquatic and soil environments, expose beneficial biological effects onto plants and act as antioxidants.[6] Recently, FA attracted substantial attention from industry while they were mentioned as a feasible source for a use as biostimulants, nominally, within a subgroup of complex carbon-based plant bio-stimulants.[7] This brought about a plethora of publications both on biostimulating properties of both HA and FA and prospects of their use in agriculture as well as on the mechanisms of biological activity exerted by HA and FA on plants.[8–10] Antioxidant activity was suggested as one of the major mechanisms which underlays biostimulating acitivity of HA and FA.[11,12]

Antioxidant properties of HS are intensively studied.[13–17] The balance between electron accepting quinones and electron donating polyphenolics is a key for antioxidant activity of HS. Still the exact structure of the antioxidant units is unknown due to extreme structural and isomeric complexity of HS as evidenced by Fourier Transform Ion Cyclotron Mass-Spectrometry (FTICR MS) studies.[18–20] Separation technologies offer a promising solution to reduce complexity of HS and selectively isolate bioactive fractions.[21–25] Reversed-phase high-performance liquid chromatography (RP-HPLC), which is traditionally used for separation of low-molecular-weight compounds by hydrophobicity, was successfully used for HS fractionation.[26] This method exploits differences in oxygenation and saturation of humic substitutents to separate complex HS mixtures.[27–29] In our previous studies, we have reported that sorption of HS onto the solid phase extraction cartridges (SPE) followed by a gradient elution with the solvents of different polarity showed good prospects for isolation of HS fractions with the enhanced biological activity such as antioxidant activity and beta-lactamase inhibiting properties.[30]

The goals of this study are twofold: firstly, we will estimate applicability of RP HPLC technique to separate peat FA into the narrow fractions with a large span of antioxidant activities; secondly, we will characterize molecular composition and optical properties of the obtained narrow fractions to better understand the relationship between molecular composition and antioxidant capacity of FA and

a.Department of Chemistry, Lomonosov Moscow State University, Leninskie Gory 1-3, 119991 Moscow, Russia. Email: khreptugova@mail.ru

View Article Online
DOI: 10.1039/D5AY00986C

for identifying analytical parameter which could be applied for identification of the fractions with enhanced antioxidant activity. For reaching the last goal we will use fluorescence measurements which are very sensitive to the balance of quinone and phenol units within the molecular ensemble of HS.

2 Experimental

2.1 Fractionation of the Fulvic Acid Sample by Preparative RP-HPLC

The parent FA material was a commercial sodium fulvate (Fulvagra WSG 90 FA) marketed by Humintech GmbH, Grevenbroich, Germany).

Chromatographic conditions were adopted from[26]. Given extensive peak overlap, we employed a generic 5–100% organic modifier gradient optimized for both resolution and throughput. The flow rate was set to the highest feasible value without exceeding the column's 30 bar pressure limit. To prepare the sample for RP-HPLC fractionation, a weight of 5.0 g of FA was dissolved in 50 mL of LC-MS grade H_2O. Fractionation was performed with a use of a GX-281 preparative RP-HPLC system (Gilson) equipped with dual binary pumps, an automated fraction collector with a 5000 µL sample loop, a UV/VIS detector set at 254 nm, and a PrepELS II evaporative light scattering detector. A ReproSil-Pur 120 C_{18}-AQ column (250 mm × 30 mm, 10 µm) with a 0.5 µm pre-column filter was used for separation. The gradient elution program mixed 0.01% formic acid in water (Solvent A) and isopropanol (IPA, Solvent B) at a flow rate of 10 mL/min to provide a gradient from 5% to 100% of IPA over 40 minutes. Fractions were collected at two-minute intervals between 8 and 40 minutes. Each fraction (120 mL) was concentrated using a Buchi Synchore Q-101 evaporator and dried to a stable mass in a CentriVap cold trap under vacuum. The fractionation scheme and a list of the collected fractions and their masses are given in Figure 1 and Table 1, respectively.

Fig. 1. Scheme of RP-HPLC fractionation of 100 g/L FA solution into 21 narrow fractions by decreasing polarity of the binary eluent composed of 0.01% formic acid in water and isopropanol.

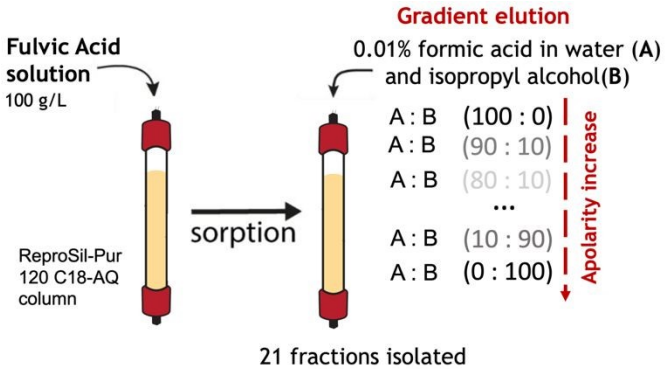

Table 1. Masses of the isolated fractions used in the study.

Fraction	% of B, isopropanol	Elution time, min	Mass, mg
Fraction 1	4	8	1017.0
Fraction 2	5	10	377.7
Fraction 3	6	12	64.9
Fraction 4	7	14	23.2
Fraction 5	8	16	82.2
Fraction 6	9	18	56.7
Fraction 7	10	20	48.9
Fraction 8	19	22	39.7
Fraction 9	28	24	34.7
Fraction 10	37	26	33.0
Fraction 11	46	28	51.1
Fraction 12	55	30	65.8
Fraction 13	64	32	77.8
Fraction 14	73	34	238.9
Fraction 15	82	36	640.7
Fraction 16	91	38	370.8
Fraction 17	100	40	62.4
Fraction 18	100	45	10.0
Fraction 19	100	50	1.9
Fraction 20	100	55	0.5
Fraction 21	100	60	0.3

The optical properties of the obtained FA fractions were characterized as described in studies of Volkov[26] using a UV-Visible Cary 4000 spectrometer (Varian, USA) and a Fluorolog-2-222 Tau spectrometer (Horiba Jobin Yvon). In brief, prior to analysis, FA fractions were reconstituted in MilliQ water at a concentration of 100 g/L and subsequently diluted to 100 mg/L for UV-Vis and to 10 mg/L for fluorescence measurements. The UV descriptors E_2/E_3 and E_4/E_6 were calculated as the ratios of optical densities at 265 nm to 365 nm and 465 nm to 665 nm, respectively, as it was suggested in literature.[31,32] Excitation-emission matrix (EEM) spectra were acquired in the range of 230-500 and 250-750 nm, respectively. The

View Article Online
DOI: 10.1039/D5AY00986E

fluorescence asymmetry values were calculated as a ratio of the "blue" band (420 to 450 nm) to "red" band (550 to 600 nm).[33]

2.2 ABTS Technique for Determination of Antioxidant Capacity of FA Fractions

The reagents - ABTS$^{\bullet+}$ (2'-azino-bis(3-ethylbenzothiazoline-6-sulfonic acid)) and Trolox (6-Hydroxy-2,5,7,8-tetramethylchromane-2-carboxylic acid) - were purchased from Sigma-Aldrich (USA). Antioxidant capacity was measured with a use of FluoStar Omega microplate reader (BMG LABTECH, Germany). MiliQ water was used for analysis. The 0.1 M citrate buffer at pH 4.0 was prepared by dissolving.[13] 76 g of citric acid and 10.15 g of sodium citrate in 1 L of MilliQ water. The results of all antioxidant assays were compared with the Trolox controls at pH 4.0 (the pH value was selected to ensure for ABTS•$^{+}$ radical stability). Each sample was tested at three concentrations with triplicate measurements per concentration and confirmed that minor pH fluctuations did not affect the reported antioxidant capacities. The measurement protocol was based on the techniques described elsewhere.[34–37] A working solution of ABTS$^{\bullet+}$ was prepared as follows: a weight of 11 mg of ABTS was dissolved in 900 µL of water. A solution of 20 mg of potassium persulfate ($K_2S_2O_8$, analytical grade, Chimmed, Russia) was prepared in 1 mL of distilled water. Subsequently, 100 µL of this solution, at a concentration of 70 µM, was added to the ABTS solution. The resulting ABTS radical stock solution (21.4 mM) was prepared at least 1 day prior to analysis and kept in the dark. Immediately prior to analysis, the stock solution was diluted with 0.1 M sodium citrate buffer at a 1:200 ratio. The initial ABTS concentration in each well was 85.6 µM. This concentration was used to calculate absorption coefficient of the ABTS radical at 734 nm for each measurement.

The quenching kinetic curves of the ABTS radical in the presence of FA or Trolox were recorded at a wavelength of 734 nm over 180 minutes (with 4 replicates). To account for ABTS radical self-quenching, observed as a slight reduction in optical density at 734 nm without addition of an antioxidant, a control kinetic curve was subtracted from each FA kinetic curve. The resulting curves were then fitted to a kinetic model, proposed by Klein et al.:[38]

$$\Delta(ABTS^{\bullet+}) = \nu\left(FA_{fast}\right)\cdot\left(1-e^{-k_{fast}\cdot C_0(ABTS^{\bullet+})\cdot t}\right)+\nu\left(FA_{slow}\right)\cdot\left(1-e^{-k_{slow}\cdot C_0(ABTS^{\bullet+})\cdot t}\right)$$

where – $\Delta(ABTS^{\bullet+})$ – the concentration change of ABTS-radical, $\nu\left(FA_{fast}\right)$ – the fast centers portion, $\nu(FA_{slow})$– the slow centers portion, k_{fast} – pseudofirst order reaction rate of the fast centers, k_{slow} – pseudofirst order reaction rate of the slow centers, $C_0(ABTS^{\bullet+})$ – initial concentration of ABTS$^{\bullet+}$ (at the moment of t = 0, t – the time of the reaction).

All kinetic curves were plotted as a function of a decrease in ABTS$^{\bullet+}$ radical concentration (ΔABTS$^{\bullet+}$) over time. The kinetic AOC value (µmol ABTS/mg FA fraction), derived from the kinetic curve fitting and determined as a sum of $\nu\left(FA_{fast}\right)$ and $\nu(FA_{slow})$, was normalized by the concentration of FA sample and then compared to a Trolox Equivalent Antioxidant Capacity (TEAC), expressed as micromoles of Trolox equivalent per milligram of FA sample (µmol/mg). To prepare the standard solution, Trolox was placed in an Eppendorf microtube and dissolved in 1500 µL of ethanol. To achieve a working concentration of 300 µM, the solution was quantitatively transferred to a 100 mL flask and diluted with MiliQ water. A series of standard solutions was prepared from the Trolox stock by aliquoting 2000, 1750, 1500, 1250, 1000, 500, and 250 µL into microtubes, and each sample was then diluted to 2 mL with citrate buffer. Subsequently, 20 µL of each solution was dispensed into three wells of a microplate, followed by the addition of 180 µL of ABTS$^{\bullet+}$ solution, and absorbance spectra were recorded. A calibration curve was then constructed based on the Trolox standards, which served to quantify the antioxidant activity of the samples in terms of Trolox equivalents. From the data obtained, the value of antioxidant activity was calculated according to the formula:

$$TEAC,mmol/g = \frac{\Delta I - b}{C\cdot a}$$

where ΔI – difference in the optical density of the control solution and the sample solution 180 minutes after the addition of the ABTS radical; C – concentration of the sample solution (g/l); a, b – coefficients calibration dependence of trolox solutions equation.

3. Results and discussion

3.1 Characteristics of Molecular Composition and Optic Properties of the FA Fractions Used in This Study

The parent FA material was fractionated by RP-HPLC technique with a use of binary mixture of 0.01% formic acid and IPA as an eluent. According to Table 1 the collected RP-HPLC fractions yielded 3.3 g out of initial 5 g of FA sample. This indicates that approximately 1.7 g of initial material remained on the column likely, due to strong interactions with the stationary phase. The highest mass (1.4 g) was eluted within the fractions FR-1-2 indicating a target isolation of more hydrophilic components in FA composition. The next drastic increase in mass eluted was observed for fractions FR-14, FR-15, FR-16, which yielded 1.25 g all together. The obtained distribution of the fraction yields suggests the presence of two largely different fractions: more hydrophilic FA and more hydrophobic FA within the parent sample of commercial FA. It should be noted that the total yield of the more hydrophobic FA fractions accounted for about 50% of the eluted material which is usually the case for isolation of more hydrophobic FA (HFA) from aquatic NOM with a use of the XAD-8 or DAX-8 resins.[39] Hence, the obtained "hydrophobic" fraction in this study might be considered as a proxy for the HFA.[39]

Given this consideration in mind, it was of interest to consider and compare molecular composition of the major "hydrophilic" (FR-1 and FR-2) and "hydrophobic" (FR-14, FR-15, FR-16) fractions. The molecular composition was calculated from the data reported.[26] The obtained data are given in Figure 2 as a ratio of the total intensities in the HR-mass-spectra of the seven major classes of HS precursors in accordance with Perminova:[40] condensed tannins, lignins (phenylisopropanoids), terpenoids, other lipids, peptides, carbohydrates, and hydrolyzable tannins.

View Article Online
DOI: 10.1039/D5AY00986C

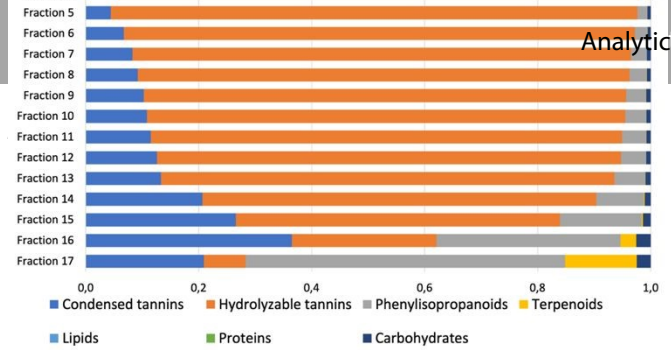

Fig. 2. Distribution of components related to chemotypes in the molecular composition of the isolated fractions.

It can be seen that the major differences in molecular compositions of more hydrophilic versus more hydrophobic fractions are reflected in the contribution of hydrolysable tannins, which completely dominate the molecular ensemble of hydrophilic fractions, versus contribution of condensed tannins and lignins, which dominate the molecular ensemble of the more hydrophobic fractions.

The optical properties of the FA fractions isolated in this study were assessed with a use of UV-Vis and fluorescence spectroscopy. The corresponding spectra are given in Figure 3.

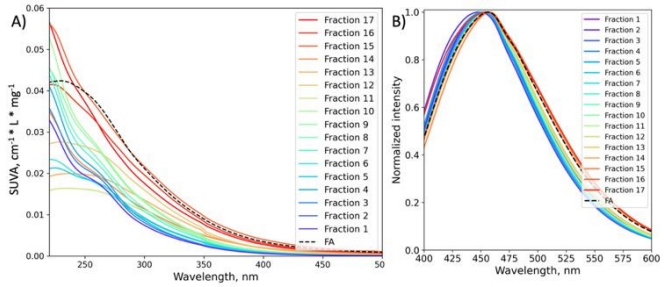

Fig. 3. UV-Vis (A) and fluorescence (B) spectra of fractions and the parent FA sample.

Figure 3A shows that the hydrophobic fractions (FR-14–17) display the highest absorbance—especially across 200–350 nm—indicating the higher content of conjugated chromophores.The obtained trend is in sync with the molecular composition data on the enrichment of the more hydrophobic fraction with the conjugated aromatic structures. Figure 3B shows the fluorescence emission spectra of the parent FA and the fractions at an excitation wavelength of 350 nm. Fluorescence spectroscopy has emerged as a valuable tool for the rapid and non-destructive characterization of organic matter as reported in previous studied.[28,41,42] Recent studies have extensively utilized the fluorescence asymmetry ratio to assess the relationship between red and blue shifts in 1D- fluorescence spectra, thereby estimating the contribution of humic-like substances with more conjugated and aromatic structures during fractionation processes.[27] Additionally, this approach has been employed to evaluate the effects of ozonation on the molecular composition of organic matter.[43] In this study a general bathochromic shift in fluorescence intensity of the fractions was observed along with an increase in IPA concentration. This motivated us to calculate fluorescence asymmetry ratio (ASM_{350}) as a proxy for the ratio of unconjugated phenols (hydrolysable tannins) contributing to blue band to the conjugated aromatics (condensed tannins and lignins) – red band. The calculated ASM_{350} values are given in Table 2 along with E_2/E_3 and E_4/E_6 values. The latter index is in use as a "humification degree" indicator,[32] whereas E_2/E_3 ratio is responsive to oxygen substitution of the aromatic ring.[31]

Table 2. Optics descriptors calculated for obtained narrow fractions and initial FA sample.

Sample	E_2/E_3	E_4/E_6	ASM_{350}
FA	5.8	5.6	4.7
Fraction 1	10.9	3.8	6.2
Fraction 2	12.5	3.6	7.2
Fraction 3	11.4	3.4	7.1
Fraction 4	12.9	2.6	6.9
Fraction 5	7.3	1.7	7.1
Fraction 6	8.5	1.7	6.5
Fraction 7	10.0	5.2	6.3
Fraction 8	9.9	4.3	6.3
Fraction 9	9.3	4.2	6.2
Fraction 10	9.3	4.3	6.1
Fraction 11	4.7	1.8	5.8
Fraction 12	5.5	2.7	5.6
Fraction 13	4.4	2.3	5.4
Fraction 14	5.5	5.7	4.6
Fraction 15	5.2	5.3	4.3
Fraction 16	5.5	4.7	4.3
Fraction 17	5.6	4.8	4.5

The E_2/E_3 ratio values decreased from 12 to 6 in the fractions eluted after the 50% IPA concentration, suggesting an increase in aromaticity and molecular weight, as previously reported in the literature.[31] The value of E_4/E_6 index remained at the low range which is related to low absorbance of fulvic acids beyond 500 nm. This fact was discussed previously in the literature in the context that substantial errors in E_4/E_6 values can be encountered by applying it to aquatic NOM or FA.[44] A rise in the E_4/E_6 values occurred after IPA content exceeded 50% indicating an increase in the content of more conjugated structures within the more hydrophobic fractions of FA. This phenomenon is in agreement with the similar trend observed in our previous publication.[45] The ASM_{350} values dropped down at the IPA concentrations above 70%. Such a behavior might be indicative of an increase in more humic-like, aromatic structures in these fractions, which was also reported in the literature.[27,33]

In conclusion, UV-visible and fluorescence spectroscopy of FA fractions indicate an optical shift toward more humified compounds with increasing IPA concentrations. A decrease in E_2/E_3 and E_4/E_6 values coupled with a fluorescence bathochromic shift, point to

View Article Online
DOI: 10.1039/D5AY00986C

increased aromaticity and conjugation in the more hydrophobic fractions of FA.

3.2 Studies on the Antioxidant Capacity of the FA Fractions Obtained in This Study

The kinetic curves of ABTS-radical quenching by the FA fractions used in this study are shown in Figure 3. Both the parent FA and all fractions are characterized with a rapid initial increase in the amount of quenched radicals (0 – 50 min) followed by a slower phase (50 – 180 min). This type of curve reflected the presence of both fast and slow antioxidant centers in the FA fractions. The more hydrophobic fractions (e.g., FR-15, FR-16), which were obtained at high IPA concentrations, displayed the most pronounced quenching rate indicating higher antioxidant potential. In contrast, the more hydrophilic fractions (e.g., FR-2) exhibited minimum scavenging ability of $ABTS^{\bullet+}$ indicative of low antioxidant capacity. The trend obtained for all FA fractions used in this study shows that the more hydrophobic fractions displayed the stronger antioxidant activity. For enabling comparison of the AOC results obtained with a use of the ABTS assay with those reported in the literature, we also measured Trolox equivalent antioxidant capacity (TEAC).[46] The obtained AOC values in Trolox equivalents are summarized in Table 3.

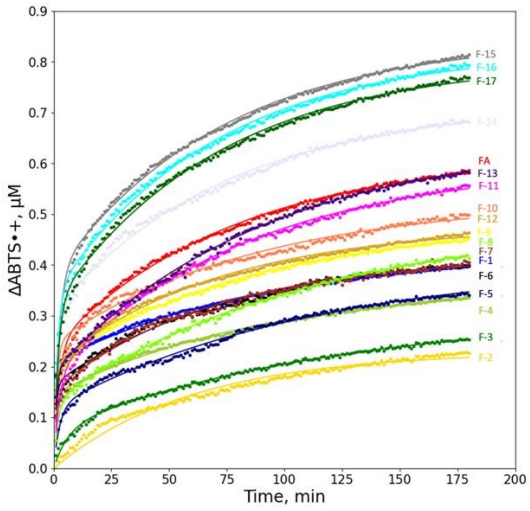

Fig. 4. Kinetic curves of ABTS radical quenching for the RP HPLC fractions of FA used in this study (the error bars stand for the standard deviation at n=3).

Table 3. TEAC-based antioxidant capacity of the parent FA and the RP-HPLC fractions.

Number of fraction	Model R^2	AOC, $ABTS^{\bullet+}$ /g	SD (n=3)	AOC, mmol TE/g	SD (n=3)
FA	0.998	0.62	0.03	0.76	0.06
1	0.923	0.52	0.04	0.52	0.06
2	0.915	0.34	0.06	0.28	0.04
3	0.992	0.32	0.02	0.22	0.08
4	0.997	0.36	0.09	0.41	0.14
5	0.995	0.41	0.04	0.38	0.05
6	0.994	0.44	0.04	0.45	0.03
7	0.993	0.42	0.05	0.46	0.06
8	0.997	0.51	0.07	0.43	0.08
9	0.997	0.48	0.05	0.57	0.05
10	0.987	0.54	0.03	0.57	0.05
11	0.998	0.60	0.03	0.69	0.06
12	0.997	0.48	0.05	0.62	0.02
13	0.996	0.66	0.02	0.73	0.06
14	0.995	0.72	0.04	0.90	0.05
15	0.997	0.85	0.09	1.03	0.10
16	0.998	0.83	0.06	1.08	0.04
17	0.998	0.75	0.05	0.93	0.08

As it can be seen, the AOC value of the parent FA was 0.76 mmol TE/g. The AOC values of the more hydrophilic fractions varied in the range from 0,2 up to 0,7 mmol TE/g, whereas the more hydrophobic FA fractions (eluted with 60% IPA and above) ranged from 0.9 to 1.14 mmol TE/g. The AOC values for the obtained fractions were consistent with previously published results. Volikov et al. (2021) reported AOC values for commercial humic substances ranging from 0.6 to 1.2 mmol TE/g.[47] The fractions isolated at the beginning of the fractionation process in this study exhibited low AOC values, comparable to those of humic acids derived from soil samples, ranging from 0.50 to 0.7 mmol TE/g. As the fractionation progressed, the AOC values of the subsequent fractions increased, more closely resembling those of fulvic acids, which are typically in the range of 1.0 to 1.2 mmol TE/g.[15] The obtained data indicate that more hydrophobic fractions exhibited markedly higher antioxidant capacities than the more polar ones showing a threefold increase in AOC overall. This increase aligns with the higher conjugated phenols content in fractions isolated with larger IPA levels during RP-HPLC. The similar trends were observed.[30] In addition, sterically hindered phenols are known for potent antioxidant potential despite slower kinetics.[48,49]

3.3 Establishing Relationships Between Antioxidant Activity of Narrow FA Fractions With Composition and Optical Indicators

The integral intensities of the seven primary chemotypes, normalized to total spectral intensity, were utilized as structural descriptors for the FA fractions in this study. Antioxidant capacity (AOC) was used as an "activity" descriptor to establish structure-activity relationships for these FA fractions. The results of the correlation analysis between

View Article Online DOI: 10.1039/D5AY00986C

the AOC parameter (mmol TE/g) and the molecular compositions of the initial FA sample and its RP-HPLC fractions are shown in Figure 5 with the correlation coefficient (r) values displayed in the corresponding chemotype on the van Krevelen diagrams (Figure 5A). As shown in Figure 5A, a significant positive correlation was observed for condensed tannins chemotype (r = 0.79), while a negative correlation was noted with hydrolysable tannins chemotype (r = -0.43). These results suggest that the AOC values of the fractions are primarily driven by a contribution of more aromatic, hydrophobic components, such as lignins and condensed tannins (hydrophobic phenolic moieties). On contrary, an increase in the contribution of oxidized, hydrophilic structures associated with hydrolysable tannins leads to a reduction in antioxidant capacity. The obtained data on the substantial role of conjugated hydrophobic structural moieties in antioxidant activity of the FA fractions used in this study are in agreement with reported trends for both non-fractionated FA and HA[13,50] and narrow fractions of HA.[30]

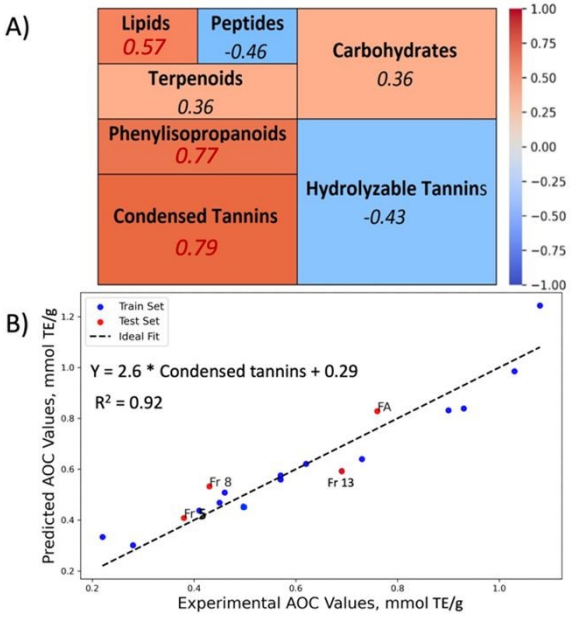

Fig. 5. Correlation and regression of antioxidant capacity against molecular chemotypes in fulvic acid and its RP-HPLC fractions(A) Heatmap of Spearman correlation coefficients between AOC (mmol TE/g) and chemotype contributions in the van Krevelen bins (positive in red, negative in blue), (B) Linear regression of predicted versus experimental AOC values for FA and its fractions (train set: blue; test set: red).

The same data set on antioxidant activity of FA fractions and molecular compositions was used to construct a predictive model based on "molecular composition – antioxidant activity" relationship as it is shown in Figure 5B. The regression equation with the highest determination coefficient (0,92) is given below:

AOC (mmol TE/g) = 2.6 × condensed tannins +0.29 (R=0.92),

where "condensed tannins" stands for the intensity-normalized population density of the van Krevelen diagram occupied by the molecular components of the "condensed tannins" chemotype.

To verify the derived predictive model, it was used to calculate the AOC parameter for four FA fractions based on the corresponding HRMS molecular composition data. The predicted values are shown with the red dots in Figure 5B. They align closely with the experimentally determined AOC (mmol TE/g) measured via ABTS radical assays supporting the robustness and reliability of the predictive model.

Principal-component analysis (PCA, Fig.6A) of the RP-HPLC fractions and the unfractionated FA resolved two main axes explaining 83 % of the variance (PC1 = 64.1 %, PC2 = 19.2 %; Figure 6A). Along PC1, fractions rich in hydrolyzable tannins, high ASM_{350}, and elevated E_2/E_3 ratios (e.g., FR-3, FR-4, FR-5) plotted strongly positive, whereas those dominated by condensed tannins and high IPA% (e.g., FR-14, FR-15) fell on the negative side. PC2 distinguished protein- and lipid-enriched fractions from IPA-dominant fractions (negative scores; aligned with the IPA vector). Notably, the condensed-tannin-rich fractions (FR-14, FR-15) also coincided with high antioxidant capacity (AOC), confirming their key role in driving FA activity. The initial FA sample occupied a distinct position at high PC2, reflecting its mixed chemotype signature.

The obtained "molecular composition - AOC" relationship led us to an idea of exploring AOC-optical properties relationships, while optics is also very sensitive to the presence of conjugated condensed tannins. In case of success, the easily measured optical parameters could be used as analytical predictors for the AOC values of FA. The best correlation relationship was established with the ASM350 parameter (R^2 = 0.96). It is shown in Figure 6B.

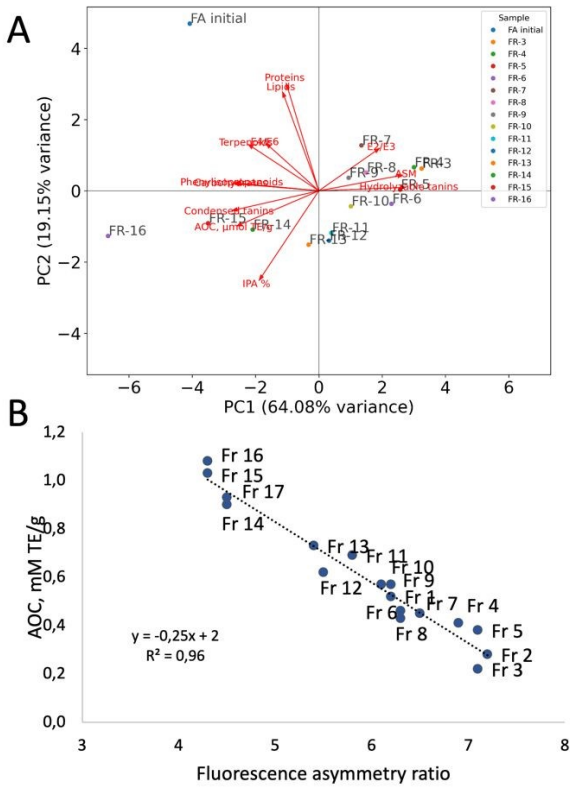

Fig. 6. A) Principal Component Analysis biplot (PC1 vs. PC2) from molecular and optical characteristics of fractions B) The fluorescence asymmetry (ASM_{350}) versus AOC value (mM TE/g) relationship for the data on all RP-HPLC FA fractions obtained in this study.

The obtained close inverse relationship between the ASM_{350} and the AOC values is indicative of a systematic increase both in the bathochromic shift of fluorescence and antioxidant activity along with an increase in the content of conjugated structures in the FA

View Article Online
DOI: 10.1039/D5AY00986C

fractions. The obtained correlation relationship based on the ASM_{350} parameter has important analytical implications: it means that simple and express 1D fluorescence measurements might be used for assessing antioxidant capacity of the FA fractions instead of a labor- and reagents - intense ABTS protocol. One-dimensional fluorescence measurements offer a reliable alternative. Of importance is that the obtained relationship was validated by direct FTICR MS measurements with regard to molecular composition of the FA fractions. Hence, the fluorescence asymmetry ratio (ASM_{350}) can be used as an optical proxy for evaluating the antioxidant activity of FA samples.

Conclusions

The conducted studies on antioxidant activities of the narrow RP-HPLC fractions of FA showed that these were more hydrophobic fractions, which exceeded in the AOC values the parent non-fractionated FA. Given that these fractions comprised about 50% by mass of the eluted material, the conclusion could be made that the RP-HPLC with water-isopropanol eluent is an efficient analytical tool for preparative isolation of the FA fractions with enhanced antioxidant activity.

Another conclusion is that HRMS provides reliable data on the content of the conjugated phenols in the FA sample which are principal drivers of the antioxidant activity of the FA fractions. The content of condensed tannins found with a use of HRMS could be used to predict the AOC value of FA sample.

It can be also concluded that the found relationship between the fluorescence asymmetry value and the antioxidant capacity of the FA sample has the most important analytical implication from the point of view of the quality control of the commercial FA materials. This relationship shows feasibility of replacing elaborate ABTS assay measurements with simple and robust fluorescence measurements. A use of asymmetry band ratio provides additional advantages by reducing demands to fluorescence spectra correction. The conducted research also opens a way for developing on-line control of the antioxidant capacity of the isolated FA fractions with a use of fluorescence detector during RP-HPLC separation of FA material.

Author contributions

Conceptualization, Dmitry Volkov and Irina Perminova; Funding acquisition, Dmitry Volkov; Investigation, Danila Gorbunov, Anna Khreptugova and Dmitry Volkov; Supervision, Irina Perminova; Visualization, Danila Gorbunov and Anna Khreptugova; Writing – original draft, Danila Gorbunov and Anna Khreptugova; Writing – review & editing, Irina Perminova.

Conflicts of interest

There are no conflicts to declare.

Data availability

Most data supporting the results are included in the article. The datasets used and/or analyzed during the current study are available from the corresponding author on reasonable request.

Acknowledgements

The authors would like to acknowledge financial support of the Russian Science Foundation grant 21-73-20202 https://rscf.ru/en/project/21-73-20202/.

Notes and references

1. F. J. Stevenson, Humus chemistry: genesis, composition, reactions, *John Wiley & Sons*, 1994.
2. E. M. Thurman, Organic geochemistry of natural waters, *Springer Science & Business Media*, 2012, vol. 2.
3. R. T. Lamar, D. C. Olk, L. Mayhew and P. R. Bloom, *J AOAC Int*, 2014, **97**, 721–730.
4. M. Schnitzer, *Can J Soil Sci*, 1967, **47**, 245–250.
5. M. Schnitzer, L. E. Lowe, J. F. Dormaar and Y. Martel, *Can J Soil Sci*, 1981, **61**, 517–519.
6. X. Tian and K. M. Schaich, *J Agric Food Chem*, 2013, **61**, 5511–5519.
7. ISO/DIS 8157(en). Fertilizers, soil conditioners and beneficial substances.
8. G. B. Conselvan, D. Pizzeghello, O. Francioso, M. Di Foggia, S. Nardi and P. Carletti, *Plant Soil*, 2017, **420**, 119–134.
9. S. Nardi, M. Schiavon, A. Muscolo, D. Pizzeghello, A. Ertani, L. P. Canellas and J. M. Garcia-Mina, *Frontiers Media SA*, 2024, preprint.
10. L. P. Canellas, F. L. Olivares, N. O. Aguiar, D. L. Jones, A. Nebbioso, P. Mazzei and A. Piccolo, *Sci Hortic*, 2015, **196**, 15–27.
11. R. T. Lamar, *The chemical biology of plant biostimulants*, 2020, 97–121.
12. R. T. Lamar, J. Gralian, W. C. Hockaday, M. Jerzykiewicz and H. Monda, *Front Plant Sci*, 2024, **15**, 1328006.
13. M. Aeschbacher, C. Graf, R. P. Schwarzenbach and M. Sander, *Environ Sci Technol*, 2012, **46**, 4916–4925.
14. B. A. G. de Melo, F. L. Motta and M. H. A. Santana, *Materials Science and Engineering: C*, 2016, **62**, 967–974.
15. O. I. Klein, N. A. Kulikova, A. I. Konstantinov, M. V Zykova and I. V Perminova, *Polymers (Basel)*, 2021, **13**, 3262.
16. M. Verrillo, M. Salzano, D. Savy, V. Di Meo, M. Valentini, V. Cozzolino and A. Piccolo, *Chemical and Biological Technologies in Agriculture*, 2022, **9**, 28.
17. M. V Zykova, I. A. Schepetkin, M. V Belousov, S. V Krivoshchekov, L. A. Logvinova, K. A. Bratishko, M. S. Yusubov, S. V Romanenko and M. T. Quinn, *Molecules*, 2018, **23**, 753.
18. M. Gonsior, J. Valle, P. Schmitt-Kopplin, N. Hertkorn, D. Bastviken, J. Luek, M. Harir, W. Bastos and A. Enrich-Prast, *Biogeosciences*, 2016, **13**, 4279–4290.
19. J. A. Hawkes, C. Patriarca, P. J. R. Sjöberg, L. J. Tranvik and J. Bergquist, *Limnol Oceanogr Lett*, 2018, **3**, 21–30.
20. D. Leyva, L. V Tose, J. Porter, J. Wolff, R. Jaffé and F. Fernandez-Lima, *Faraday Discuss*, 2019, **218**, 431–440.
21. T. A. Brown, B. A. Jackson, B. J. Bythell and A. C. Stenson, *J Chromatogr A*, 2016, **1470**, 84–96.
22. I. V Perminova, A. I. Konstantinov, E. V Kunenkov, A. Gaspar, P. Schmitt-Kopplin, N. Hertkorn, N. A. Kulikova and K. Hatfield, *Biophysico-Chemical Processes Involving Natural Nonliving Organic Matter in Environmental Systems*, 2009, 487–538.

23. Y. Qin, M. Zhang, W. Dai, C. Xiang, B. Li and Q. Jia, *Fitoterapia*, 2019, **137**, 104270.
24. I. A. Schepetkin, G. Xie, M. A. Jutila and M. T. Quinn, *Phytotherapy Research: An International Journal Devoted to Pharmacological and Toxicological Evaluation of Natural Product Derivatives*, 2009, **23**, 373–384.
25. A. C. Stenson, B. M. Ruddy and B. J. Bythell, *Int J Mass Spectrom*, 2014, **360**, 45–53.
26. D. S. Volkov, S. M. Byvsheva and M. A. Proskurnin, *Environ Sci Technol*, 2024, **58**, 20444–20456.
27. A. Zherebker, E. Shirshin, A. Rubekina, O. Kharybin, A. Kononikhin, N. A. Kulikova, K. V Zaitsev, V. A. Roznyatovsky, Y. K. Grishin and I. V Perminova, *Environ Sci Technol*, 2020, **54**, 2667–2677.
28. K. R. Murphy, S. A. Timko, M. Gonsior, L. C. Powers, U. J. Wunsch and C. A. Stedmon, *Environ Sci Technol*, 2018, **52**, 11243–11250.
29. P. Herzsprung, N. Hertkorn, W. Von Tümpling, M. Harir, K. Friese and P. Schmitt-Kopplin, *Anal Bioanal Chem*, 2016, **408**, 2461–2469.
30. T. A. Mikhnevich, V. G. Grigorenko, M. Y. Rubtsova, G. D. Rukhovich, S. Yiming, A. N. Khreptugova, K. V Zaitsev and I. V Perminova, *ACS Omega*, 2023, **9**, 1858–1869.
31. G. V Korshin, C.-W. Li and M. M. Benjamin, *Water Res*, 1997, **31**, 1787–1795.
32. Y. Chen, N. Senesi and M. Schnitzer, *Soil science society of America journal*, 1977, **41**, 352–358.
33. A. Zsolnay, E. Baigar, M. Jimenez, B. Steinweg and F. Saccomandi, *Chemosphere*, 1999, **38**, 45–50.
34. I. G. Munteanu and C. Apetrei, *Int J Mol Sci*, 2021, **22**, 3380.
35. N. Walpen, M. P. Lau, A. Fiskal, G. J. Getzinger, S. A. Meyer, T. F. Nelson, M. A. Lever, M. H. Schroth and M. Sander, *Environ Sci Technol*, 2018, **52**, 11151–11160.
36. R. Re, N. Pellegrini, A. Proteggente, A. Pannala, M. Yang and C. Rice-Evans, *Free Radic Biol Med*, 1999, **26**, 1231–1237.
37. C. Bravo, M. De Nobili, A. Gambi, L. Martin-Neto, O. R. Nascimento and R. Toniolo, *Chemosphere*, 2022, **286**, 131755.
38. O. I. Klein, N. A. Kulikova, I. S. Filimonov, O. V Koroleva and A. I. Konstantinov, *J Soils Sediments*, 2018, **18**, 1355–1364.
39. ISO 19822, 2018. Fertilizers and soil conditioners — Determination of humic and hydrophobic fulvic acids concentrations in fertilizer materials.
40. I. V Perminova, *Pure and Applied Chemistry*, 2019, **91**, 851–864.
41. A. Stubbins, J.-F. Lapierre, M. Berggren, Y. T. Prairie, T. Dittmar and P. A. del Giorgio, *Environ Sci Technol*, 2014, **48**, 10598–10606.
42. C. Zhao, Z. Wang, C. Wang, X. Li and C.-C. Wang, *Environmental pollution*, 2018, **243**, 177–188.
43. P. Aguilar-Alarcón, A. Zherebker, A. Rubekina, E. Shirshin, M. A. Simonsen, J. Kolarevic, C. C. Lazado, E. N. Nikolaev, A. G. Asimakopoulos and Ø. Mikkelsen, *Science of The Total Environment*, 2022, **843**, 157009.
44. N. Senesi, T. M. Miano, M. R. Provenzano and G. Brunetti, *Science of The Total Environment*, 1989, **81**, 143–156.
45. I. V Perminova, E. A. Shirshin, A. I. Konstantinov, A. Zherebker, V. A. Lebedev, I. V Dubinenkov, N. A. Kulikova, E. N. Nikolaev, E. Bulygina and R. M. Holmes, *Environ Sci Technol*, 2018, **52**, 12526–12537.
46. I. R. Ilyasov, V. L. Beloborodov and I. A. Selivanova, *Chemical Papers*, 2018, **72**, 1917–1925.
47. A. B. Volikov, N. V Mareev, A. I. Konstantinov, A. A. Molodykh, S. V Melnikova, A. E. Bazhanova, M. E. Gasanov, E. N. Nikolaev, A. Y. Zherebker and D. S. Volkov, *Agronomy*, 2021, **11**, 2047.
48. J. L. Munoz-Munoz, F. Garcia-Molina, R. Varon, J. Tudela, F. Garcia-Canovas and J. N. Rodriguez-Lopez, *J Agric Food Chem*, 2010, **58**, 2062–2070.
49. A. S. Pannala, T. S. Chan, P. J. O'Brien and C. A. Rice-Evans, *Biochem Biophys Res Commun*, 2001, **282**, 1161–1168.
50. A. B. Volikov, N. V Mareev, A. I. Konstantinov, A. A. Molodykh, S. V Melnikova, A. E. Bazhanova, M. E. Gasanov, E. N. Nikolaev, A. Y. Zherebker and D. S. Volkov, *Agronomy*, 2021, **11**, 2047.

View Article Online
DOI: 10.1039/D5AY00986C

Data availability

Most data supporting the results are included in the article. The datasets used and/or analyzed during the current study are available from the corresponding author on reasonable request.